
Modeling and simulation of Polysiloxane diaphragm pressure sensor whit graphene beam

Mohamed Elmahdi Ali

Electrical Department, Engineering College /Sirte University, Libya

*Crosspnding author: shaglouf@su.edu.ly

Abstract:

This paper studies a resonant pressure sensor whose elementary sensing component is the polysiloxane circular diaphragm, and the final sensing component is the graphene beam resonator attached to the polysiloxane circular diaphragm. The relationship between the fundamental natural frequency of the beam resonator and the measured pressure is calculated. As the beam is located at different positions of the upper plane of the polysiloxane circular diaphragm along its radial direction is a simulation, analyzed, and investigated. Some significant results are obtained. . Based on the differential output frequencies, a set of optimum parameters of the proposed Pressure Sensor is determined. The performed pressure range is 0~10Kpa. Keywords: polysiloxanee , beam, pressure; graphene; Frequency.

Introduction

Microelectromechanical systems are systems that consist of small-scale electrical and mechanical components for specific purposes. MEMS were translated into systems with mechanical and electrical components but have extended their boundaries to include optical, radio-frequency, and Micro devices [1].

The resonant sensor is based on a special sensing structure, which is operating at its resonating state. And the measured quantities can be detected by using the resonant frequency (or the natural frequency), phase shift, or amplitude of the vibrating output signal for the sensing component [2].

resonant pressure sensors have been widely used in the automotive industry, medical instrument, aerospace, and military fields due to their high accuracy, long-term stability, direct digital output (without A/D conversion), low hysteretic, and high repeatability[3].

Polysiloxane is composed of atoms arranged in a diamond structure with a cubic symmetry. Although Polysiloxane has a tendency to cleave along crystallographic planes because of the bulk defects in the crystal, it is a mechanical material with high strength [4].

Graphene is a one-atom-thick layer of carbon atoms arranged in a hexagonal lattice. Graphene is the thinnest material known to man at one atom thick, and also incredibly strong - about 200 times stronger than steel. On top of that, graphene is an excellent conductor of heat and electricity[5].

Sensors are devices used to measure physical or chemical states. They deliver a signal that can be received by a machine or person. As a rule, the measurements (the reactions of the sensor element to the states to be measured) are converted into electrical or optical signals and, namely, increasingly into digital signals. Optical glass fibers are gaining growing importance in the transmission of signals [6].

Circular diaphragm sensors are one of the more sophisticated elementary sensing components of Polysiloxane microstructure resonant sensors when compared to square diaphragm sensors. The following are its main benefits: stress concentration on the useful ring sensing area, adjustable stress distribution design, simpler attainment of a differential measurement scheme to boost sensitivity and minimize some disturbances, such as temperature, etc. This paper's goal is to demonstrate a sophisticated Polysiloxane resonant pressure sensor model created using the finite element technique (FEM). The link between the output frequency and the applied pressure is simulated and calculated using the model [7].

SENSOR STRUCTURE AND OPERATING PRINCIPLE

Fig. 1 shows the structure of a Pressure sensor. The preliminary sensing unit is a polysiloxane circular diaphragm. The pressure being measured acts perpendicularly on the lower plane of the circular diaphragm and yields circumferential and radial stresses. The final sensing unit is a graphene beam attached to the upper plane of the circular diaphragm. The thickness of the diaphragm H should be much greater than the Thickness of the beam h.

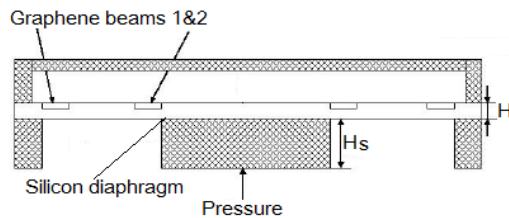


Fig.1 sensing structure of the pressure sensor

Based on the structural characteristics, the beam's axial direction is subjected to an appropriate beginning stress that is equal to the radial stress of the circular diaphragm at the same location. The natural frequency of the graphene beam varies with the radial stress on the upper plane of the polysiloxane circular diaphragm because the primary vibration of the beam occurs along its normal direction (direction of the beam's thickness) and the initial stress is applied along the axial direction of the beam (direction of the beam's length). Therefore, the change in the beam's inherent

frequency will be used to determine the applied pressure.

STRESSES ON THE UPPER PLANE OF POLYSILOXANE CIRCULAR DIAPHRAGM

The circular diaphragm loaded by pressure at its center has the following differential equation: [8].

$$\frac{d}{dr} = \left[\frac{1}{r} \frac{d}{dr} \left(r \frac{dw}{dr} \right) \right] = \frac{G}{\lambda} \quad (1)$$

$$\lambda = \frac{EH^3}{12(1-\mu^2)}, \quad G = \frac{rP}{2}$$

Where:-

P - the applied Pressure ($P \geq 0$).

λ - the flexural rigidity of the diaphragm.

W-the normal displacement of the circular diaphragm.

E-The Young's modulus.

μ -the Poisson ratio of the sensing structure.

G = the shearing force at the circumference of radius r of the diaphragm.

The boundary conditions at the inner and outer edges of the circular diaphragm are as follows

$$\begin{cases} r = R_1 & \frac{dw}{dr} = 0 \\ r = R_2 & w \frac{dw}{dr} = 0 \end{cases} \quad (2)$$

Where:-

r - radial coordinate of the circular diaphragm in polar.

From Eqs. (1) and (2), the normal displacement of the circular diaphragm W can be obtained.

Then the radial stress $\sigma_r(r)$ and circumferential stress $\sigma_\theta(r)$ of the circular diaphragm can be obtained as follows [8].

$$\begin{cases} \sigma_r(r) = \frac{-3PA^2}{8H^2} \left[(3+\mu)R^2 - (1+\mu)(K^2+1) - \frac{(1-\mu)K^2}{R^2} \right] \\ \sigma_\theta(r) = \frac{-3PA^2}{8H^2} \left[(1+3\mu)R^2 - (1+\mu)(K^2+1) + \frac{(1-\mu)K^2}{R^2} \right] \end{cases} \quad (3)$$

$$R = \frac{r}{R_2}, \quad K = \frac{R_1}{R_2}$$

ANALYTICAL ANALYSIS AND SIMULATION OF GRAPHENE BEAM

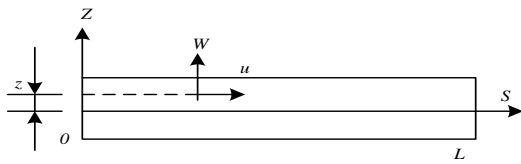


Fig.2 The model of graphene beam

Fig. 2 shows the mathematical model of the beam. The axial and normal vibrating displacements $u(s,z,t)$ and $w(s,t)$ of the beam at an arbitrary point in Cartesian coordinates can be written as [9].

$$\begin{cases} u(s, z, t) = -z \frac{dw(s)}{ds} \cos \omega t \\ w(s, t) = w(s) \cos \omega t \end{cases} \quad (4)$$

Where:-

s, z - the axial and normal coordinates of the beam in Cartesian coordinates.

ω [rad/s] - the natural frequency.

$w(s)$ - Corresponding vibrating shape along the axial direction of the beam.

Then the finite element equation is as follows

$$(K - \omega^2 M)a = 0 \quad (5)$$

Where:-

K- assembly stiffness Matrix.

M- assembly Mass Matrix

a - the assembly nodal vector, consisting of all a_j .

For the actual structural features of Fig.2, the boundary conditions of the beam are as follows

$$\begin{cases} s = 0: & w(s) = w'(s) = 0 \\ s = L: & w(s) = w'(s) = 0 \end{cases} \quad (6)$$

Eq.(5) is the FEM model for the microstructure polysiloxane resonant Pressure sensor shown in Fig. 1. From Eqs. (5) and (6) the natural frequencies and their corresponding vibrating shapes can be obtained.

SENSOR PRESSURE DETECTION CIRCUIT SYSTEM

The pickup signals is very weak and lost in the loud background noise because the size of the resonant beam and vibration amplitude is so small [9]. A detection circuit system is created based on the lock-in amplify principle to extract the weak vibrating signal. It carries out tests for the pressure sensor's characteristics. The circuit system's block diagram is shown in Figure 3.

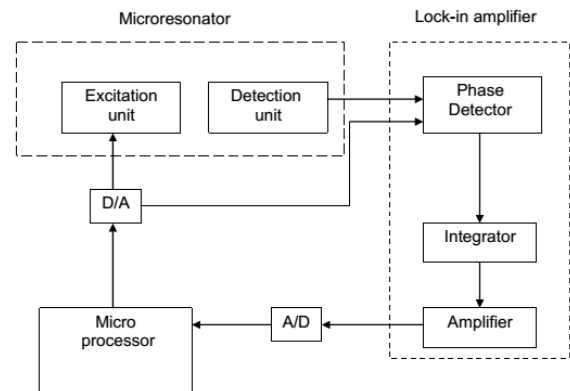


Fig.3. The block diagram of the detection circuit system

CALCULATION AND DISCUSSION

In this paper, the main investigations are the varying laws of the Pressure-frequency relationship for the graphene beam resonator as the thickness H , inner radius R_1 for the polysiloxane circular diaphragm and the corresponding lengths of the graphene beam L are varied. In order to get some generalized results of the pressure -frequency relationship for the graphene beam resonator, some related parameters are selected as follows:

The Reference value for the outer radius of the circular diaphragm is $R_2 = 4 \times 10^{-3} m$. Reference values for the width and thickness of the beam are $b = 10 \times 10^{-5} m$ and $h = 1 \times 10^{-5} m$.

INVESTIGATION OF THE FREQUENCY-PRESSURE RELATIONSHIP

Define $f(P)$, $f(0)$ the basic natural frequency of the beam for pressure P and for pressure; $P = 0$; $\Delta f = f(P) - f(0)$ as the variation of the basic natural frequency of the beam within $(0, P)$ and $\beta = [f(P) - f(0)] / f(0)$ [%] as the relative variation or the sensitivity of the basic natural frequency for the beam within $(0, P)$ the interval.

LOCATION OF BEAM ON THE UPPER PLANE OF THE CIRCULAR DIAPHRAGM

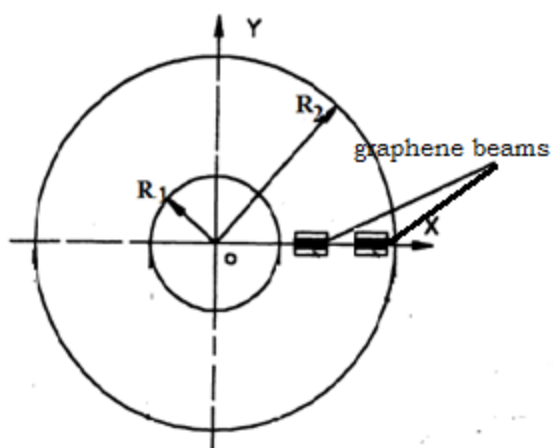


Fig.4 the upper plane of the polysiloxane circular diaphragm

The frequency changes of the two graphene beams are opposite, one is positive, and the other is negative. Therefore, the differential output scheme can be realized, and the measured Pressure can be determined by the frequency difference between beam 2 and beam 1.

The distance $R_2 - R_1 - 2L$ (fig 4) between beam2 and beam1 could not be selected as too small compared with the length of the beam L. On the other hand, in order to make use of the effective annular sensing area of the polysiloxane circular diaphragm, the distance $R_2 - R_1 - 2L$ could not be selected too big. In this paper, the relationship for R_2, R_1 , and L is selected as

$$R_2 - R_1 = 2.3L \quad (7)$$

In such a case, the length of the beam L is dependent on the inner radius of the polysiloxane circular diaphragm R_1 .

Table1 gives the beam’s relationships between frequency and measured Pressure within 0-10Kpa, as the beam is located at different positions.

Table2 gives the frequency variation and sensitivity of the beam corresponding to Table

Table 1: The frequency of graphene beam within 10KPa

Pressure M Pa	Location of the beam		
	1.4 ,2.47	2.21,3.2	2.98,4
0.0	645.714	645.714	645.714
1	661.484	639.799	615.276
2	684.188	641.532	591.674
3	706.198	643.241	567.126
4	727.472	644.834	541.448
5	748.148	646.483	514.426
6	768.272	647.997	486.004
7	787.787	649.452	456.074
8	806.933	650.914	423.938
9	825.499	652.300	389.409
10	856.479	665.719	364.604

Table 2: The variation frequency and sensitivity of graphene beam within 10K pa

Position	1.4 ,2.47	2.21,3.2	2.98,4
Sensitivity	32.6 %	3.1 %	-43.5 %
Variation(kHz)	210.765	20.005	-281.110

From the Tables, some results can be obtained as follows:

As the beam is located at different positions of the upper plane of the diaphragm along its radial direction, the sensitivity of the beam resonator is different.

The best location for the beam resonator is at the inner edge and the outer edge for the

circular diaphragm, where the beam's sensitivity reaches the biggest.

The beam resonator is defined as beam1 as it is located at the outer edge, and defined as beam2 as the beam located at the inner edge.

THE THICKNESS OF THE POLYSILOXANE CIRCULAR DIAPHRAGM

The thickness of the polysiloxane circular diaphragm H should be much greater than the Thickness of the graphene beam h., fig. 5 shows the relationships between the frequency of beam1 and the pressure for the different thicknesses of the diaphragm H. Fig. 6 shows the relationships between the frequency of beam2 and the pressure for the different thicknesses of the diaphragm H.

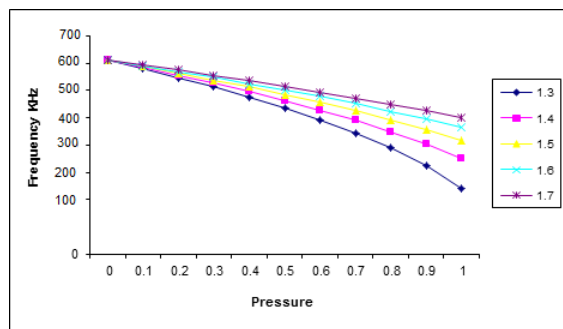


Fig. 5:The relationships between the frequency of beam1 and the pressure

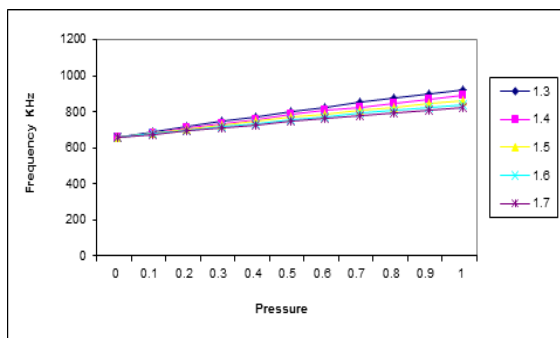


Fig.6: The relationships between the frequency of beam2 and the pressure

Table 3: The variation frequency (kHz) of Beam1 and Beam2

H ($\times 10^{-4}$ m)	$(R_1 \times 10^{-5}$ m, $L \times 10^{-4}$ m)			
	Beam1		Beam2	
	(1.35,1.06)	(1.4,1.04)	(1.35,1.06)	(1.4,1.04)
1.3	-503.261	-472.812	275710	281.228
1.4	-381.451	-365.721	251.842	246.003
1.5	-302.217	-294.789	206.508	206.236
1.6	-251.103	-245.781	189.463	185.125
1.7	-219.493	-213.681	167.530	165.372

Table 4:The Sensitivity of Beam1 and Beam2

H ($\times 10^{-4}$ m)	$(R_1 \times 10^{-5}$ m, $L \times 10^{-4}$ m)			
	Beam1		Beam2	
	(1.35,1.06)	(1.4,1.04)	(1.35,1.06)	(1.4,1.04)
1.3	-70.7 %	-69.5 %	40.3 %	39.7 %
1.4	-55.2 %	-51.9 %	37.4 %	34.8 %
1.5	-45.5 %	-43.7 %	31.3 %	28.9 %
1.6	-37.9 %	-36.6 %	26.3 %	26.2 %
1.7	-32.6 %	-30.1 %	25.2 %	24.5 %

From the tables and figures, we can get the following results:

The relative frequency variation (sensitivity) is increased as the thickness of the polysiloxane circular diaphragm H decreases for beam1 and beam2.

The relative frequency variation (sensitivity) is increased as the inner radius of the polysiloxane circular diaphragm R_1 decreases or the length of the beam increases for beam1 and beam2.

DESIGN AND OPTIMIZED PARAMETERS FOR PRESSURE SENSOR

Based on the differential output scheme of the Pressure Sensor and some related criteria, a set of appropriate parameters for the sensing structure of the sensor is determined for measuring the Pressure within 0-10 K Pa.

Outer radius R_2	$4 \times 10^{-3} \text{m}$
Inner radius R_1	$1.35 \times 10^{-3} \text{m}$
Thickness H	$1.4 \times 10^{-4} \text{m}$
Length of beam L	$1.06 \times 10^{-4} \text{m}$
Width of beam b	$10 \times 10^{-5} \text{m}$
Thickness of beam h	$1 \times 10^{-5} \text{m}$
frequency range for beam 1	(645.714-364.604)khz
frequency range for beam 2	(645.714-856.479)khz

CONCLUSIONS

The modelling and simulation for a Pressure Sensor are carried out in this paper. The elementary sensing component of the Pressure Sensor is the Polysiloxane circular diaphragm, and its final sensing component is the graphene beam resonator which is attached to the Polysiloxane circular diaphragm. The sensitivity of the basic natural frequency to measure Pressure for the beam resonator will be increased as the thickness of the circular diaphragm H being decreased, or the inner radius of the circular diaphragm R_1 is decreased, as the outer radius keeping constant, or the length of the graphene beam being increased. It is the best selection for a pair of beams (beam 1 and beam 2) to be located at the outer and inner edges of the circular diaphragm, respectively.

References

[1] S, Shanky, R Sharma, B. D. (2021). Design and development of MEMS based guided beam type piezoelectric energy harvester. Springer Singapore. . online]. Available at: www.libgen.io

[2] Duqi, Enri, Giorgio Allegato, and Mikel Azpeitia. "Pressure Sensors." *Silicon Sensors and Actuators*. Springer, Cham, 2022. 523-541.

[3] Y , Zhuoqing. (2021). Advanced MEMS/NEMS Fabrication and Sensors. Springer International Publishing AG. Available at: www.libgen.io

[4] Osipov, Artem A., et al. "Silicon carbide dry etching technique for pressure sensors design." *Journal of Manufacturing Processes* 73 (2022): 316-325.

[5] Liu, Jihong, Siyu Bao, and Xinzhe Wang. "Applications of Graphene-Based Materials in Sensors: A Review." *Micromachines* 13.2 (2022): 184.

[6] ZHAO, Wen-sheng, et al. "A Review on Microwave Resonant Sensors." *ACTA ELECTONICA SINICA* (2022): 1.

[7] E, Masayoshi, ed, (2021). 3D and Circuit Integration of MEMS. online]. Available at www.libgen.io

[8] M. Shaglouf, A. Abugalia, Finite Element Modeling and Simulation of A Microstructure Quartz Beam Resonant, Sirte University Scientific Journal (Applied Sciences), Vol. 8 (1), 113–120 June 2018

[9] M. Shaglouf s.omer. Modeling and simulation and fabrication of resonant pressure sensor with silicon nitride beam. Third International Conference on Electrical Engineering and Information technology (ICEEIT 2021), 30 31 October 2020, Benghazi – Libya.

[10] Dhanaselvam, P. Suveetha, et al. "Pressure Sensors Using Si/ZnO Heterojunction Diode." *Silicon* 14.8 (2022): 4121-4127.

[11] Belwanshi, Vinod, Sebin Philip, and Anita Topkar. "Performance Study of MEMS Piezoresistive Pressure Sensors at Elevated Temperatures." *IEEE Sensors Journal* 22.10 (2022): 9313-9320.

[12] Tai, Guojun, et al. "Force-Sensitive Interface Engineering in Flexible Pressure Sensors: A Review." *Sensors* 22.7 (2022): 2652.

[13] Ha, Kyoung-Ho, et al. "Soft Capacitive Pressure Sensors: Trends, Challenges, and Perspectives." *ACS nano* 16.3 (2022): 3442-3448.

[14] Wang, Lukang, et al. "Development of Laser-Micromachined 4H-SiC MEMS Piezoresistive Pressure Sensors for Corrosive Environments." *IEEE Transactions on Electron Devices* 69.4 (2022): 2009-2014.

[15] Kim, Youn, et al. "Fabrication of highly conductive graphene/textile hybrid electrodes via hot pressing and their application as piezoresistive pressure sensors." *Journal of Materials Chemistry C* 10.24 (2022): 9364-9376.